Grip-pattern verification for a smart gun

Xiaoxin Shang
Raymond N. J. Veldhuis
University of Twente
Signals and Systems Group
Electrical Engineering
P. O. Box 217
7500 AE Enschede
The Netherlands
E-mail: x.shang@utwente.nl

Abstract. *In the biometric verification system of a smart gun, the rightful user of the gun is recognized based on grip-pattern recognition. It was found that the verification performance of grip-pattern recognition degrades strongly when the data for training and testing the classifier, respectively, have been recorded in different sessions. The major factors that affect the verification performance of this system are the variations of pressure distribution and hand position between the probe image and the gallery image of a subject. In this work, three methods are proposed to reduce the effect of the variations by using different sessions for training, image registration, and classifier fusion. Based on these methods, the verification results are significantly improved. © 2008 SPIE and IS&T.*
[DOI: 10.1117/1.2892675]

1 Introduction

Our work focuses on the development of a prototype recognition system as part of a smart gun with grip-pattern recognition, ensuring that it can only be fired by its rightful user. The smart gun is intended for use by the police, since carrying a gun in public brings considerable risks. In the United States, vital statistics show that about 8% of the law-enforcement officers killed in a shooting incident were shot by their own weapons.[1] Biometric authentication is an attractive solution to this problem, because it requires minimal or no additional action by the user. This approach has been taken up by a small number of parties, both industrial and academic, who proposed a number of solutions. In Ref. 2, an authentication system based on voice verification is described. The drawback of such a system is that it is not reliable in noisy environments. Solutions based on fingerprint recognition have been described in Ref. 3, for example. The disadvantage of fingerprint recognition on a pistol is that it does not work in combination with gloves and that it is sensitive to dirt and weather conditions.

Grip-pattern recognition, i.e., recognition based on the pressure exerted when holding an object, does not have these disadvantages. This type of biometric recognition has been investigated by the New Jersey Institute of Technology,[4,5] by Belgian weapon manufacturer FN Herstal, and by us.[6–12] The only results reported, besides ours, were published in Ref. 5, which is different from the one reported here in various aspects. First, in Ref. 5, the dynamics of the grip-pattern prior to firing are used, while in our approach recognition is, at present, based on a static grip pattern. Second, in Ref. 5, 16 pressure sensors are used: one on the trigger, and 15 on the grip of the gun. These sensors are piezo-electric sensors, producing 16 time signals. We apply a much larger resistive sensor array, which produces a pressure image. Third, the recognition methods of both systems differ. In Ref. 5, a method based on neural networks is presented, which seems to be trained for identification, whereas we apply likelihood-ratio-based verification.[13] Another difference is the way that both systems have been evaluated. In Ref. 5, data was collected from four shooters, while we used data from 39 trained police officers, who are the targeted user group. The recognition results are, unfortunately, difficult to compare because in Ref. 5 the recognition rates obtained in an identification experiment were presented, while we present equal error rates in a verification experiment, which is more relevant for the final application.

The first prototype of our grip-pattern recognition system has been described in Refs. 6 and 7 in terms of its design, implementation, and evaluation. The sensor, used for measuring the grip pattern, is a 44×44 piezo-resistive pressure sensor made by Tekscan Incorporated, South Boston.[14] An initial collection of grip patterns was gathered from a group of mostly untrained subjects with no experience in shooting. Figure 1 shows both the prototype of the smart gun and an example of a grip pattern. From Fig. 1(b), one can see the pressure pattern of the thumb in the upper-left part of the image and those of the other fingers in the lower-left part. Note that only three fingers are present, because the index finger is on the trigger of the gun. First experimental results indicated that the grip pattern contained useful information for identity verification.[7]

To explore the verification performance of the system when used by its target user, the police, we have collected new data from a group of police officers in three sessions with one month and four months in between, approximately. The data have been processed for verification by using the recognition algorithm described in Refs. 7 and 11. The experimental results indicate that if data for training and testing come from the same session, the verification results are fairly good, with an equal-error rate (EER) of

Paper 07098SSR received Jun. 14, 2007; revised manuscript received Oct. 11, 2007; accepted for publication Oct. 18, 2007; published online Mar. 19, 2008.
1017-9909/2008/17(1)/011017/9/$25.00 © 2008 SPIE and IS&T.

Downloaded From: https://www.spiedigitallibrary.org/journals/Journal-of-Electronic-Imaging on 21 Mar 2022
Terms of Use: https://www.spiedigitallibrary.org/terms-of-use

(a)

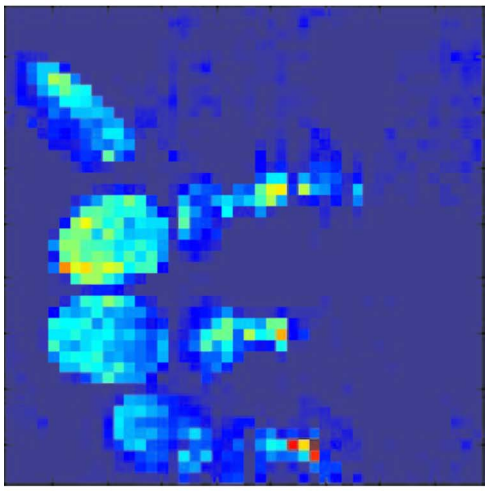

(b)

Fig. 1 (a) Prototype of the smart gun. (b) An example of grip-pattern image.

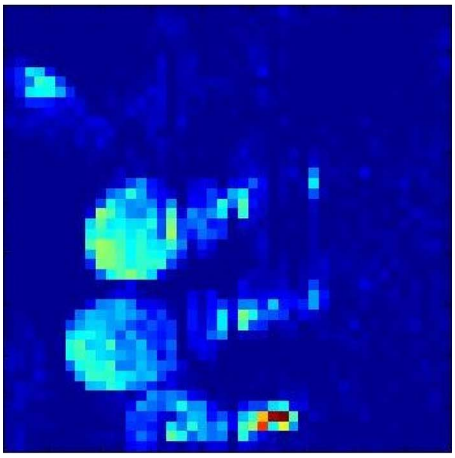

(a)

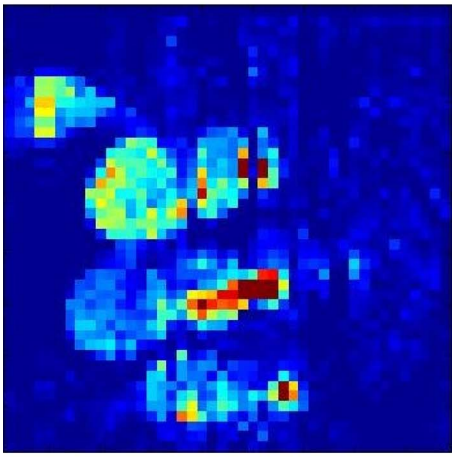

(b)

Fig. 2 Grip-pattern images of a subject in different sessions.

below 1%. If data for training and testing come from different sessions, with weeks or more in between, the results are unsatisfactory, i.e., about 15% EER on average. The EER is the false-accept rate (FAR), or false-reject rate (FRR), at the point of operation of the verifier where the FAR equals the FRR. Since in practice there will always be a time interval between data enrollment and verification, the across-session results are more realistic, and therefore, need to be improved.

After analyzing the images collected in different sessions, we have found that even though the grip-pattern images from a certain subject collected within one session look fairly similar, a subject tends to produce data with larger variations across sessions. First, a variation of pressure distributions occurs between grip patterns from a subject across sessions. Second, another type of variation results from the hand shift of a subject. Figure 2 shows two images collected from one subject in two different sessions, respectively. One can see that these two images have quite different pressure distributions. Also, the grip pattern in Fig. 2(b) is located higher than that in Fig. 2(a). Further research has shown that these variations are the main reason for the unsatisfactory across-session verification results.[11] Therefore, to improve the recognition results, the effect of the across-session variations of data needs to be reduced.

First, we have combined the data of two out of three sessions for training to model the across-session variations in the training procedure better, and we have used data of the remaining session for testing. This has brought significant improvement of the recognition results. Second, to further reduce the variation caused by the hand shift, we have applied template-matching registration (TMR)[15] as a preprocessing step prior to classification. For comparison, maximum-matching-score registration (MMSR)[11] has also been implemented. It has been found that TMR is able to effectively improve the across-session verification results, while MMSR is not. However, the hand shift measured by MMSR has proved particularly useful in discriminating impostors from genuine users. If two images belong to the same subject, the hand shift value produced by MMSR is on average much smaller than if they belong to different subjects. This has inspired the design of a new classifier, based on both the grip pattern and the hand shift. The verification error rates have been further reduced significantly.

Downloaded From: https://www.spiedigitallibrary.org/journals/Journal-of-Electronic-Imaging on 21 Mar 2022
Terms of Use: https://www.spiedigitallibrary.org/terms-of-use

Table 1 Within-session experimental results.

Session	EER(%)
0	1.4
1	0.5
2	0.8
3	0.4

Table 2 Across-session experimental results.

Train	Test	EER (%)
2	1	5.5
3	1	14.7
1	2	7.9
3	2	20.2
1	3	24.1
2	3	19.0

This work presents and analyzes methods to improve the verification performance of the system. Section 2 describes the verification algorithm. Subsequently, the procedure of data collection is reviewed in Sec. 3. Section 4 presents and analyzes the experimental results. Finally, conclusions are given in Sec. 5.

2 Verification Algorithm

It is assumed that the data are Gaussian. The verification is based on a likelihood-ratio classifier. The likelihood-ratio classifier is optimal in the Neyman-Pearson sense, i.e., the FAR is minimal at a given FRR or vice versa, if the data have a known probability density function.[13,16] The pixels in the 44×44 image containing the grip pattern have values in the range [0…255], corresponding to a pressure range of 0…30 psi.[6] These pixel values are arranged into a (in this case $44\times44=1936$-dimensional) column vector $\mathbf{x}$. Prior to classification, the measurement vector $\mathbf{x}$ is normalized, i.e., $\|\mathbf{x}\|_2=1$, and subsequently each element $\mathbf{x}_i$ is replaced by $\log(x_i+\epsilon)$, with $\epsilon=10^{-16}$ added to prevent problems if $x_i=0$. The reason for the normalization is that it makes the verifier robust to global pressure variations. The reason for taking the logarithm is that the probability density function (PDF) of the data better approximates a Gaussian PDF.

A measured grip pattern originates either from a genuine user, or from an impostor. The grippattern data of a certain subject is characterized by a mean vector $\boldsymbol{\mu}_W$ and a covariance matrix $\boldsymbol{\Sigma}_W$, where the subscript W denotes "within-class," while the impostor data is characterized by $\boldsymbol{\mu}_T$ and $\boldsymbol{\Sigma}_T$, where the subscript T denotes "total." The underlying thought is that we assume that no further assumptions can be made about an impostor. Therefore, the impostor data are drawn from the density of all possible grip patterns, which is called the total density. The matching score of a measurement $\mathbf{x}$ with respect to this subject is derived from the log-likelihood ratio. It is computed by

$$S(\mathbf{x}) = -(\mathbf{x}-\boldsymbol{\mu}_W)^T\boldsymbol{\Sigma}_W^{-1}(\mathbf{x}-\boldsymbol{\mu}_W) + (\mathbf{x}-\boldsymbol{\mu}_T)^T\boldsymbol{\Sigma}_T^{-1}(\mathbf{x}-\boldsymbol{\mu}_T). \tag{1}$$

The superscript T denotes vector or matrix transposition. If $S(\mathbf{x})$ is a preset threshold, the measurement is accepted as being from the genuine user. Otherwise it is rejected. The threshold determines the FRR and the FAR of the verification.

In practice, the mean vectors and covariance matrices are unknown, and need to be estimated from a set of training data. In our case, the number of training samples from each subject should be much greater than 1936. Otherwise, the algorithm would become overtrained, and estimates of $\boldsymbol{\Sigma}_T$ and $\boldsymbol{\Sigma}_W$ would be inaccurate. In fact, as a rule of thumb, it is recommended to use at least ten times as many training examples as the number of parameters to be estimated.[17] Clearly, we could not possibly acquire such a large number of measurements. This problem was solved by the following steps prior to classification. First, we whiten the data by means of principal component analysis (PCA), such that $\boldsymbol{\Sigma}_T$ becomes an identity matrix with a reduced dimensionality of N_{PCA}. At this point we make a simplifying assumption that all subjects share the same within-class covariance matrix, so that it can be estimated more accurately from the data of all the subjects. It has been proved in Ref. 7 that in this new feature space, the number of modes of variations contributing to the verification is not more than $N_{\mathrm{user}}-1$, where N_{user} is the number of subjects in the training data. Moreover, these modes of variations are those with the smallest variances. Accordingly, a further dimensionality reduction is achieved by applying another orthogonal transform to the data, thus diagonalizing the within-class covariance matrix, and subsequently discarding all the modes of variations except the $N_{\mathrm{user}}-1$ ones with the smallest variances. This last operation is in fact a dimensionality reduc-

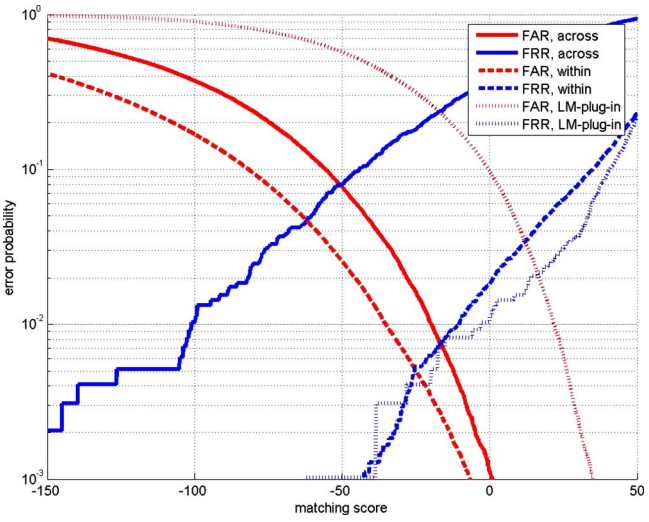

Fig. 3 FAR and FRR curves obtained from across-session, within-session, and LM-plug-in experiments. Session 1 was used for training, session 2 for testing.

Downloaded From: https://www.spiedigitallibrary.org/journals/Journal-of-Electronic-Imaging on 21 Mar 2022
Terms of Use: https://www.spiedigitallibrary.org/terms-of-use

Table 3 Across-session experimental results in EER (%) with one entity estimated from subset B.

Train	2	3	1	3	1	2
Test	1	1	2	2	3	3
RF	5.5	14.7	7.9	20.2	24.1	19.0
$\boldsymbol{\mu}_w$	1.0	2.2	2.1	2.8	2.7	2.6
$\boldsymbol{\Lambda}_W$	6.0	13.5	7.3	17.3	24.3	19.9
$\boldsymbol{\mu}_T$	5.5	14.9	8.0	20.0	24.0	19.2
F	3.8	23.8	3.2	18.3	13.7	14.9

tion by means of linear discriminant analysis (LDA). After LDA, the total covariance matrix remains an identity matrix, while the within-class covariance matrix becomes diagonal. Both covariance matrices have a dimensionality of $N_{\mathrm{LDA}}=N_{\mathrm{user}}-1$.[7] The whole procedure of dimensionality reduction can be represented by a multiplication by a transformation matrix $\mathbf{F}$. As a result, Eq. (1) can be rewritten as

$$S(\mathbf{x}) = -(\mathbf{p}-\mathbf{q})^T\boldsymbol{\Lambda}_W^{-1}(\mathbf{p}-\mathbf{q}) + (\mathbf{p}-\mathbf{r})^T(\mathbf{p}-\mathbf{r}), \tag{2}$$

where

$$\mathbf{p} = \mathbf{F}\mathbf{x}, \tag{3}$$

$$\mathbf{q} = \mathbf{F}\boldsymbol{\mu}_W, \tag{4}$$

$$\mathbf{r} = \mathbf{F}\boldsymbol{\mu}_T, \tag{5}$$

and $\boldsymbol{\Lambda}_W$ denotes the resulting diagonal within-class covariance matrix. Therefore, a total of four entities needs to be estimated from the training data: $\boldsymbol{\mu}_W$, $\boldsymbol{\mu}_T$, $\mathbf{F}$, and $\boldsymbol{\Lambda}_W$. The reader is referred to Ref. 7 for more details of the verification method.

3 Data Collection

We have recorded the grip-pattern data from a group of police officers in three sessions,[8] with approximately one and four months in between. In total, 41 subjects have participated in both the first and second sessions with 25 grip-pattern images recorded from each subject. Data from two subjects have not been used in the experiments in this work, because the image quality was insufficient. In the third session, however, data have been collected from 22 subjects out of the same group and each subject contributed 50 images.

In each session, the subject was asked to pick up the gun, aim it at a target, hold it, say "ready" as a signal for us to record his grip-pattern image, and then release the gun after the recording was finished. For each subject, this procedure has been repeated for the recording of all the samples.

Table 4 Across-session experimental results with double-trained model.

Train	Test	EER(%)
2+3	1	4.0
1+3	2	5.1
1+2	3	13.7

4 Experiments, Results and Discussion

4.1 *Initial Experiments*

4.1.1 *Experiment setup and results*

Two types of experiments have been done. One is the within-session experiment, in which data for training and testing are clearly separated but come from the same session. The other is the across-session experiment, in which data collected in two different sessions are used for training and testing, respectively. The verification performance is evaluated by the overall EER of all the subjects. The EER is the false-accept rate (FAR), or false-reject rate (FRR), at the point of operation of the verifier where the FAR equals

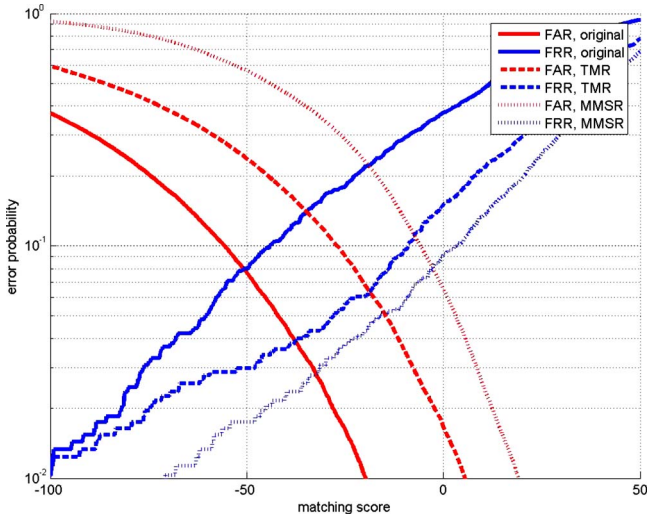

Fig. 4 FAR and FRR curves obtained from the across-session experiments with and without registration approaches.

Downloaded From: https://www.spiedigitallibrary.org/journals/Journal-of-Electronic-Imaging on 21 Mar 2022
Terms of Use: https://www.spiedigitallibrary.org/terms-of-use

Table 5 Across-session experimental results in EER (%) with and without registration approaches.

Train	2	3	1	3	1	2
Test	1	1	2	2	3	3
RF	5.5	14.7	7.9	20.2	24.1	19.0
TMR	3.9	12.9	6.0	17.8	18.4	18.9
MMSR	5.8	17.7	8.0	22.9	27.7	22.8

the FRR. It is computed from the likelihood ratios of all the genuine users and impostors. In the within-session experiment, the overall EER is computed based on all the likelihood ratios obtained from 20 runs. In each single run, 75% of the data are randomly chosen for training and the remaining 25% for testing. The number of dimensions retained after the PCA step (see Sec. 2) is given by $N_{\mathrm{PCA}}=75$. This number was obtained experimentally and is not very critical. The number of features after the LDA step was given by $N_{\mathrm{LDA}}=N_{\mathrm{user}}-1$. This means that $N_{\mathrm{LDA}}=38$ when data from the first and second sessions were used for training, and $N_{\mathrm{LDA}}=21$ when data from the third second session was used.

The results are presented in Table 1. As a reference, the result obtained with data collected from a group of untrained subjects who have no experience in shooting is also presented, denoted as session 0. Table 2 shows the across-session experimental results. The corresponding FAR and FRR curves are shown in Fig. 3. Here, as an example, the data from the first and second sessions are used for training and testing, respectively.

One can see that if data for training and testing come from the same session, the verification results are fairly good. Also, much lower error rates have been obtained with data from the police officers, compared to the case where data have been collected from the untrained subjects. However, much worse verification results were produced when data collected in two different sessions were used for training and testing, respectively.

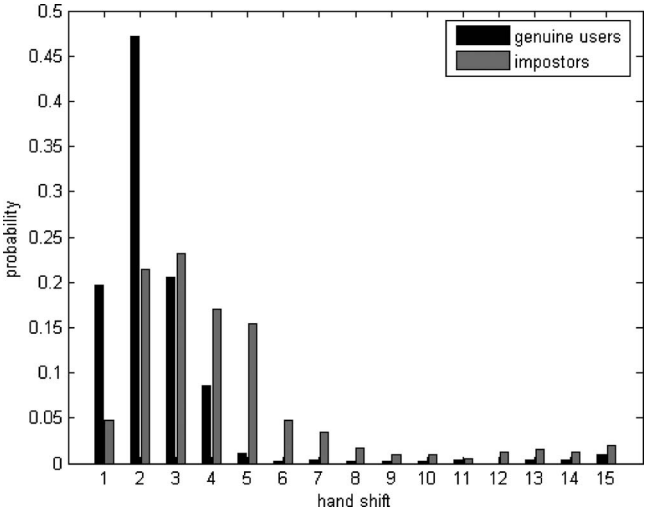

Fig. 5 Probability distributions of hand shift after TMR.

4.1.2 *Data characteristics*

Comparing the grip-pattern images of one subject recorded in different sessions, we have found large across-session variations. That is, the grip pattern of a certain subject seems to vary greatly from one session to another. See Fig. 2 for an illustration of this effect. Specifically, two types of variations have been observed. First, the pressure distribution of one's data recorded in one session is usually quite different from that recorded in another session. Second, the hand position changes from one session to another.

As a result of the across-session variations of data, the value of each entity in Sec. 2 ($\boldsymbol{\mu}_W$, $\boldsymbol{\mu}_T$, $\mathbf{F}$, and $\boldsymbol{\Lambda}_W$) varies from session to session. To find out the variation of which entity affects the verification performance the most, we did the following "plug-in" experiment. First, we randomly split the test set into two subsets of equal size, denoted as A and B, then we use one subset, for example, A, for testing. In the computation of Eq. (2), each time we estimate three out of the four entities from the training set, yet the fourth one from subset B.

The experimental results are given in Table 3, in which the last four rows contain the EERs obtained with $\boldsymbol{\mu}_W$, $\boldsymbol{\mu}_T$, $\mathbf{F}$, and $\boldsymbol{\Lambda}_W$ estimated from subset B. As a reference, the original EERs of the across-session verification are also shown, denoted as RF. Obviously, the across-session variation in $\boldsymbol{\mu}_W$, the mean value of each individual subject's data, affects the verification performance the most. If this type of variation is reduced, the verification results improve dramatically and become much closer to those shown in

Table 6 Across-session experimental results in EER (%) with double-trained model, with and without registration approaches.

Train	2+3	1+3	1+2
Test	1	2	3
RF	4.0	5.1	13.7
TMR	3.2	5.5	13.1
MMSR	4.4	7.7	20.1

Downloaded From: https://www.spiedigitallibrary.org/journals/Journal-of-Electronic-Imaging on 21 Mar 2022
Terms of Use: https://www.spiedigitallibrary.org/terms-of-use

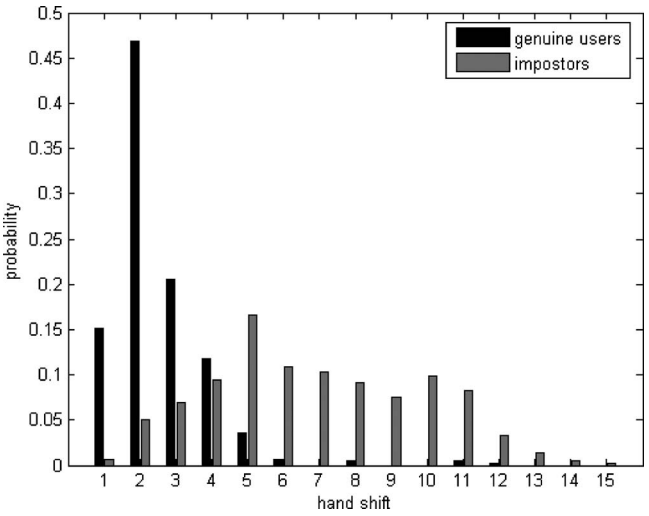

Fig. 6 Probability distributions of hand shift after MMSR.

Table 1. The error rates before and after "plugging in" the mean values are shown in Fig. 3. It can be observed that the FRR has decreased compared with the across-session case. On the other hand, the FAR has increased. However, this effect is not as strong as that of the decrease of FRR.

4.2 *Experiments with a Double Trained Model*

Given the previous analysis, the verification results can be improved by reducing the across-session variations in the mean value of each subject's data. Therefore, we combine data of two out of the three sessions for training and use data of the remaining session for testing. In this way, both the variation of the pressure distribution and that of the hand position are modeled much better in the training procedure, compared to the case where the classifier is trained on only one session of data. Table 4 shows the experimental results. One can see that great improvement has been achieved, compared to those shown in Table 2.

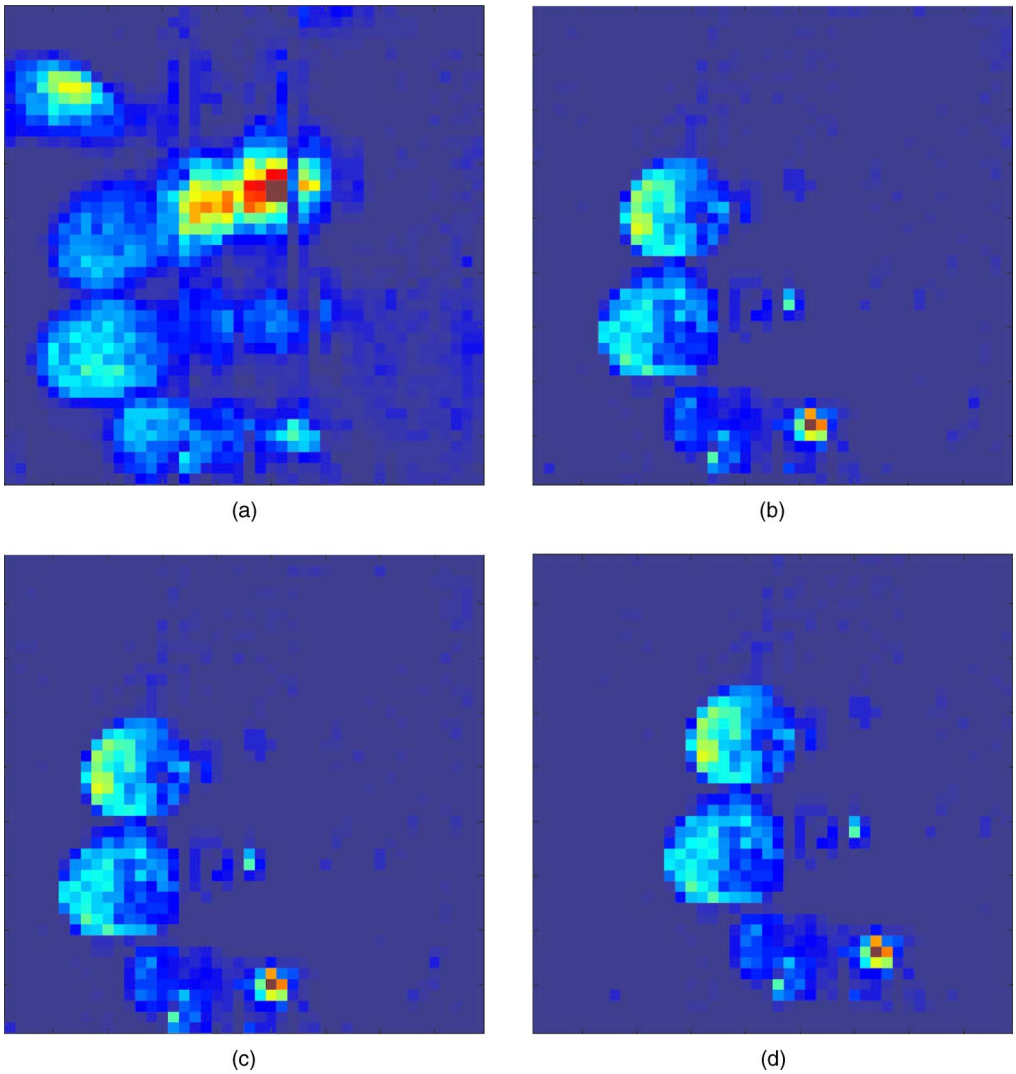

Fig. 7 (a) Template image of one subject from the first session; (b) image of an impostor from the second session; (c) image of the impostor after TMR; and (d) image of the impostor after MMSR.

Downloaded From: https://www.spiedigitallibrary.org/journals/Journal-of-Electronic-Imaging on 21 Mar 2022
Terms of Use: https://www.spiedigitallibrary.org/terms-of-use

Table 7 Across-session experimental results in EER (%) with reference and improved classifiers.

Train	2	3	1	3	1	2
Test	1	1	2	2	3	3
RF	5.5	14.7	7.9	20.2	24.1	19.0
TMR	3.9	12.9	6.0	17.8	18.4	18.9
COM	3.4	8.1	5.0	12.4	11.0	12.6

4.3 *Experiments with Data Registration*

To reduce the data variation caused by the hand shift further, we apply data registration as a preprocessing step prior to classification. According to our observation, only translation is relevant in the grip-pattern image registration. Two registration methods are concerned: template-matching registration (TMR) and maximum-matching score registration (MMSR). We first introduce these approaches. The experimental results by using them are compared afterward.

4.3.1 *Registration method description*

In TMR,[15] the cross correlation of a measured image and a registration-template image is computed. The location of the pixel of the highest value in the output image determines the hand shift value of the measured image with respect to the template image. If the measured image is well aligned regarding the template image, this pixel should be located precisely in the origin of the output image. In our case, the measured image, the template image, and the output image are all of the same size, i.e., 44×44. The shifted version of an original image after TMR can be described as

$$\mathbf{x}_0 = \arg\max_{\tilde{\mathbf{x}}} \frac{\mathbf{y} \cdot \tilde{\mathbf{x}}}{\|\mathbf{y}\|\|\tilde{\mathbf{x}}\|}, \tag{6}$$

where $\tilde{\mathbf{x}}$ denotes a shifted version of an original image $\mathbf{x}$, and $\mathbf{y}$ denotes the template image for registration.

In MMSR, a measured image is aligned to such a position that the maximal matching score, $S(\mathbf{x})$ in Eq. (2), is obtained. Specifically, an image is shifted pixel by pixel in both the horizontal and vertical directions. After each movement, a new matching score is computed. This procedure continues until the original image has been shifted to all the possible locations within a predefined scope of 20 pixels in each direction. In the end, the shifted image with the maximal matching score is selected as the registration result. It can be represented as

$$\mathbf{x}_0 = \arg\max_{\tilde{\mathbf{x}}} \mathrm{S}(\tilde{\mathbf{x}}), \tag{7}$$

where $\tilde{\mathbf{x}}$ denotes a shifted version of the original image $\mathbf{x}$.

4.3.2 *Experimental results after registration*

Prior to classification, we applied TMR and MMSR to the test data, respectively. Note that in both cases TMR was applied to the training data to build up a stable after-registration model with user-specific registration templates. Specifically, among all the training samples of a certain subject, the one with the minimal Euclidean distance to their mean value was used as the registration template of this subject. This procedure was repeated iteratively until no more shift occurred for each image. Also, we only used the lower-left part, of size 33×33, of each image, where the fingers of the subjects are located, to compute the cross

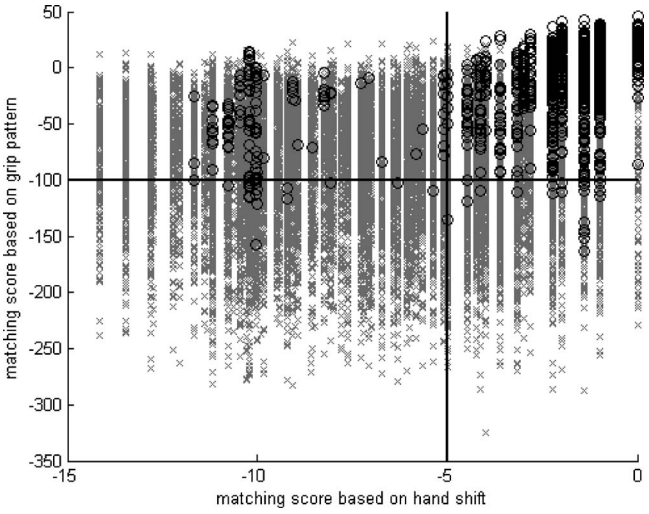

Fig. 8 Scatter graph of matching scores computed from both grip pattern and hand shift.

Table 8 Across-session experimental results in EER (%) with double-trained model, with reference and improved classifiers.

Train	2+3	1+3	1+2
Test	1	2	3
RF	4.0	5.1	13.7
TMR	3.2	5.5	13.1
COM	2.3	4.5	9.5

Downloaded From: https://www.spiedigitallibrary.org/journals/Journal-of-Electronic-Imaging on 21 Mar 2022
Terms of Use: https://www.spiedigitallibrary.org/terms-of-use

correlation. There are several reasons for this. First, for a certain subject, sometimes the positions of the thumb and fingers do not always change in the same way (see Fig. 2). Second, according to our observation, sometimes the pressure pattern of one's thumb is rather unclear or not even present, and therefore, not reliable enough for the registration.

Tables 5 and 6 present the experimental results. As a reference, the results without any data registration are also shown, represented as RF. One can see that except in one case in Table 6, the results have been improved when TMR is applied to the test data, while the results become worse when the test data are preprocessed by MMSR.

The corresponding FAR and FRR curves can be found in Fig. 4. In this figure, the data from the first and second sessions were used for training and testing, respectively. One can see that when either of the two registration methods is in use, for a certain threshold of the matching score, FRR decreases and FAR increases compared to their counterparts without any registration step. However, in the case of TMR, FRR decreases more than FAR increases, while in the case of MMSR it is the other way around.

The different effects of these registration methods result from their working principles and the characteristics of the grip-pattern images. Apart from the hand shift, a large variation of the pressure distribution may exist between a measured grip pattern and the template to which it is compared (see Fig. 2). Therefore, neither of the registration methods may yield an ideal result. Note that in TMR the "template image" refers to the *registration* template image, while in MMSR it refers to the *recognition* template image, i.e., $\boldsymbol{\mu}_W$ in Eq. (2). The increase in EER when MMSR is applied, shown in Table 5, may be explained as follows. Since the original matching scores of the impostors will be relatively low compared to those from the genuine users, the increase in the matching scores of the impostors will be on average larger than of the genuine users. That is, the effect of the increasing FAR will be stronger than that of the decreasing FRR. In contrast, TMR, not aiming at a maximum matching score, does not increase the FAR as much as MMSR does. As a net effect, TMR improves the verification results, whereas MMSR does not.

4.4 *Verification Based on Both Grip Pattern and Hand Shift*

For each measured image, the application of both TMR and MMSR results in a value of hand shift. We found that if the measured image and the template image belong to the same subject, the produced hand shift value is on average much smaller than if they belong to two different subjects, respectively. This is easy to understand, since the variations of data from two different subjects are supposed to be more than those from the same subject. Therefore, it is very likely that the grip pattern of the impostor needs to be shifted more than that of the genuine user to obtain the highest matching score. As an example, Figs. 5 and 6 present the probability distributions of the l^2-norm of the hand shifts as measured by TMR and MMSR, respectively. The training data are from the third session, and the test data are from the first session. One can see that the hand shifts from the impostors are generally small values in Fig. 5, yet those in Fig. 6 are much more wildly distributed. From these figures it can be observed that genuine and impostor hand shifts are more discriminative if they are produced by MMSR rather than by TMR. Specifically, the hand shifts from the impostors produced by MMSR are on average larger than those produced by TMR, while the hand shifts from the genuine users have similar values produced by these two approaches. This may be because the registration results of TMR depend more on the global shapes of the grip patterns, which constrains the shift values of the images from impostors to a relatively small value. See Fig. 7 for an illustration of this effect.

Inspired by the special characteristic of the hand shift produced by MMSR, we implemented a new classifier as a combination of two classifiers. Specifically, one is based on the grip pattern by using the current recognition algorithm, with TMR as a preprocessing step. The other one performs the verification based on the minus l^2-norm, obtained from the hand shifts in both the vertical and horizontal directions produced by MMSR. Note that in both classifiers, TMR is applied to the training data to build up a stable after-registration model. A measured grip-pattern image is verified as being from the genuine user if, and only if, the verification results given by both classifiers are positive.[18,19]

This can be interpreted by Fig. 8, where circles and stars represent images from the genuine users and the impostors, respectively. Let the threshold value be set as -5 on the horizontal axis, and as -100 on the vertical axis. Then only those corresponding images, represented as scatter points located in the upper-right corner on the plot, will be classified as being from the genuine user, while all the other images will be rejected.

Tables 7 and 8 show that the verification results have been further improved by using the combination of these two classifiers, denoted as COM. For easy comparison, the experimental results in the third and the fourth rows of Table 5 are presented as well.

5 Conclusion

The grip pattern has been proved to contain useful information for identity verification. However, due to large variations of each subject's data collected in different sessions, the recognition performance of the system is not yet satisfactory. There are mainly two types of variation. One is the variation of pressure distributions. The other type of variation results from the hand shift of the subject.

To improve the verification results, we first apply the double-trained model. The data of two sessions are combined for training, so that the variations can be modeled better in the training procedure. In this way, significant improvement of the verification results is achieved. Second, two registration approaches are applied to further reduce the variation caused by the hand shift: template-matching registration (TMR) and maximum-matching score registration (MMSR). Both methods prove to be useful to improve the verification performance of the system. Specifically, verification error rates are reduced effectively when the TMR is used as a preprocessing step prior to classification. Also, the hand shift value produced by the MMSR is on average much smaller if the measured image and the template image belong to the same subject rather than if they belong to two different subjects, respectively. As a result, a

Downloaded From: https://www.spiedigitallibrary.org/journals/Journal-of-Electronic-Imaging on 21 Mar 2022
Terms of Use: https://www.spiedigitallibrary.org/terms-of-use

new classifier is designed based on both the grip patterns preprocessed by TMR, and the hand shifts produced by MMSR. The application of this combined classifier has greatly improved the verification results further.

Acknowledgments

This research is supported by the Technology Foundation STW, applied science division of NWO, and the technology programme of the Ministry of Economic Affairs.

References

1. The National Uniform Crime Reporting Program, "Law enforcement officers killed and assaulted," Tech. Rep., Federal Bureau of Investigation, Washington D.C. (2001).
2. G. T. Winer, "Gun security and safety system," U.S. Patent No. 5,459,957 (Oct. 1995).
3. H. B. Adams, "Safety trigger," U.S. Patent No. 5,603,179 (Feb. 1997).
4. M. Recce, "Unauthorized user prevention device and method," U.S. Patent No. 6,563,940 (May 2003).
5. T. Chang, Z. Chen, B. Cheng, M. Cody, M. Liska III, W. Marshall, M. Recce, D. Sebastian, and D. Shishkin, "Enhancing handgun safety with embedded signal processing and dynamic grip recognition," *Proc. IECON 2005, 31st Ann. Conf. IEEE Industrial Electron. Soc.*, pp. 2107–2113 (2005).
6. J. A. Kauffman, A. M. Bazen, S. H. Gerez, and R. N. J. Veldhuis, "Grip-pattern recognition for smart guns," in *Proc. ProRISC 2003, 14th Ann. Workshop Circuits, Syst. Signal Process.*, pp. 379–384 (2003).
7. R. N. J. Veldhuis, A. M. Bazen, J. Kauffman, and P. H. Hartel, "Biometric verification based on grip-pattern recognition," *Proc. SPIE*, 5306, 634–641 (2004).
8. X. Shang, R. N. J. Veldhuis, A. M. Bazen, and W. P. T. Ganzevoort, "Algorithm design for grip-pattern verification in smart gun," in *Proc. ProRISC 2005, 16th Ann. Workshop Circuits. Syst. Signal Process.*, pp. 674–678 (2005).
9. I. R. Buhan, A. M. Bazen, P. H. Hartel, and R. N. J. Veldhuis, "A false rejection oriented threat model for biometric systems," *Advances Biometrics, Intl. Conf. (ICB2006)* 3832, 728–736, Springer Verlag, Berlin (2006).
10. X. Shang, K. Kooi, R. N. J. Veldhuis, and W. P. T. Ganzevoort, "Restoration of missing lines in grip-patterns for biometrics," *Proc. 6th IEEE Benelux Signal Process. Symp. (SPS-2006)*, pp. 95–98 (2006).
11. X. Shang and R. N. J. Veldhuis, "Registration of hand-grip pattern in smart gun," in *Proc. ProRISC 2006, 17th Annu. Workshop Circuits, Syst. Signal Process.*, pp. 192–195 (2006).
12. I. R. Buhan, J. M. Doumen, P. H. Hartel, and R. N. J. Veldhuis, "Feeling is believing: a secure template exchange protocol," *Advances Biometrics, Intl. Conf. (ICB2007)* 4642, 897–906, Springer Verlag, Berlin (2007).
13. H. L. Van Trees, *Detection, Estimation, and Modulation Theory*, Wiley, New York (1968).
14. W. L. Maness *et al.*, "Pressure and contact sensor for measuring dental occlusion," United States Patent No. 4,856,993 (Aug. 1989).
15. A. Jain, *Fundamentals of Digital Image Processing*, Prentice-Hall, Englewood Cliffs, NJ (1989).
16. A. M. Bazen and R. N. J. Veldhuis, "Likelihood-ratio-based biometric verification," *IEEE Trans. Circuits Syst. Video Technol.* **14**, 86–94 (Jan. 2004).
17. A. K. Jain, R. P. W. Duin, and J. Mao, "Statistical pattern recognition: a review," *IEEE Trans. Pattern Anal. Mach. Intell.* **22**, 4–37 (Jan. 2000).
18. C. Ji and S. Ma, "Combinations of weak classifers," *IEEE Trans. Neural Netw.* **8**(1), 32–42 (Jan. 1997).
19. L. Xu, A. Krzyzak, and C. Y. Suen, "Methods of combining multiple classifiers and their applications to handwriting recognition," *IEEE Trans. Syst. Man Cybern.* **22**(3), 418–435 (May/June 1992).

Xiaoxin Shang received her BSc degree in electrical engineering from Northwestern Polytechnic University, China, in June 2001. In March 2004 she received the MSc degree in electrical engineering from the Telecommunication Group, University of Twente, The Netherlands. Since August 2004 she has been working as a PhD student in the Signals and Systems Group, University of Twente, The Netherlands. She has been working on the secure grip project. Her research domain is biometrics and pattern recognition.

Raymond N. J. Veldhuis received his engineering degree in electrical engineering in 1981 from the University of Twente, The Netherlands. In 1988 he received the PhD degree from Nijmegen University. From 1982 until 1992 he worked as a researcher at Philips Research Laboratories in Eindhoven in various areas of digital signal processing, such as audio and video signal restoration and audio source coding. From 1992 until 2001 he worked at the Institute of Perception Research, Eindhoven, in speech signal processing and speech synthesis. He is now an associate professor at Twente University, working in the fields of biometrics, pattern recognition, and signal processing.

Downloaded From: https://www.spiedigitallibrary.org/journals/Journal-of-Electronic-Imaging on 21 Mar 2022
Terms of Use: https://www.spiedigitallibrary.org/terms-of-use